Navigational strategies underlying temporal phototaxis in *Drosophila* larvae

Running title: Temporal phototaxis in *Drosophila* larvae

Maxwell L. Zhu[1,2], Kristian J. Herrera[2,3], Katrin Vogt[1,3], and Armin Bahl[2,3,*]

[1] Department of Physics, Harvard University, 17 Oxford Street, Cambridge, MA 02138, USA

[2] Department of Molecular and Cellular Biology, Harvard University, 16 Divinity Avenue, Cambridge, MA 02138, USA

[3] Center for Brain Science, Harvard University, 52 Oxford Street, Cambridge, MA 02138, USA

*Correspondence: arminbahl@fas.harvard.edu

Keywords: *Drosophila* larvae, behavior, navigation, phototaxis, modeling

Summary statement

Using a novel closed-loop behavioral assay, we show that *Drosophila* larvae can navigate light gradients exclusively using temporal cues. Analyzing and modeling their behavior in detail, we propose that larvae achieve this by accumulating luminance change during runs.

Abstract

Navigating across light gradients is essential for survival for many animals. However, we still have a poor understanding of the algorithms that underlie such behaviors. Here we develop a novel phototaxis assay for *Drosophila* larvae in which light intensity is always spatially uniform but constantly updates depending on the location of the animal in the arena. Even though larvae can only rely on temporal cues in this setup, we find that they are capable of finding preferred areas of low light intensity. Further detailed analysis of their behavior reveals that larvae initiate turns more frequently and that turn amplitudes become higher when animals experience luminance increments over extended periods of time. We suggest that temporal integration of luminance change during runs is an important – and so far largely unexplored – element of phototaxis.

Introduction

Finding the preferred location or a particular sensory cue in complex natural environments is a computational challenge for many animals. Such taxis behaviors include chemotaxis, where animals seek or avoid chemical stimuli; thermotaxis, where animals aim to find cooler or warmer regions; and phototaxis, where animals approach or avoid light (Gepner et al., 2015; Gomez-Marin and Louis, 2014; Gomez-Marin et al., 2011; Kane et al., 2013; Klein et al., 2015; Luo et al., 2010). During these behaviors, the environment offers the animal both spatial information, such as a temperature cline across the animal's body or luminance differences in its visual field of view, as well as temporal information, for instance, a change in chemical concentration over time following a motor action. However, under most natural conditions it is difficult to disentangle whether the animal is utilizing spatial or temporal cues to guide its behavior.

Drosophila larvae are negatively phototactic throughout most of their development, preferring darker regions to brighter regions (Sawin et al., 1994). When presented with a spatially differentiated light landscape, larvae alternate between runs and turn events – during runs, larvae move relatively straight, while during turn events they sweep their heads from side to side to choose a new moving direction (Lahiri et al., 2011). As they sweep their heads, larvae might use light-sensitive receptors on their head to actively sample local asymmetries across space (Humberg and Sprecher, 2018; Humberg et al., 2018; Kane et al., 2013) to make motor decisions (Gomez-Marin and Louis, 2012; Kane et al., 2013). However, it is still unclear whether such local spatial information is necessary for *Drosophila* larvae to perform phototaxis behaviors. For example, it has been shown that zebrafish larvae can perform phototaxis in a virtual luminance landscape in which light intensity is uniform across space but changes over time according to the position of the animal (Chen and Engert, 2014). In such a purely temporal phototaxis assay, any spatial information about luminance is absent. Therefore, these animals likely use some form of temporal integration of luminance cues to navigate these environments.

Previous work indicates that as the global brightness of their environment increases over time, larvae will respond with more turn events and higher turn angles (Humberg et al., 2018; Kane et al., 2013). Moreover, during chemotaxis, larvae experiencing a decrease in the concentration of a favorable odorant over several seconds are more likely to initiate a turn (Gomez-Marin et al., 2011). However, it remains unclear whether such behavioral modulations are sufficient for *Drosophila* larvae to ably navigate a temporally variant but spatially uniform environment.

Here we set out to test if *Drosophila* larvae can perform temporal phototaxis. Using a virtual landscape in which luminance is always spatially uniform but depends on the location of the

animal, we find that larvae can navigate towards their preferred location, the darker region. Further dissections of the behavior reveal that they likely do so by integrating luminance change during runs and that such cues increase the likelihood of initiating a turn event.

Materials and methods

Experimental setup

All experiments were performed using wild-type second-instar *Drosophila melanogaster* larvae collected 3–4 days after egg-laying. Larvae were raised on agarose plates with grape juice and yeast paste, with a 12h/12h light-dark cycle at 22 °C and 60% humidity. Before experiments, larvae were washed in several droplets of deionized water. All experiments were carried out between 2 pm and 7 pm to avoid circadian effects (Mazzoni et al., 2005).

Larvae were placed in the center of a circular acrylic dish (6 cm radius) filled with a thin layer of freshly made 2% agarose. For closed-loop tracking and presentation of visual stimuli, we used a system that was originally developed for the study of larval zebrafish behavior (Bahl and Engert, 2020). In brief, spatially uniform whole-field illumination was presented via a projector (60 Hz, AAXA P300 Pico Projector, light intensity from 0 to 120 Lux) from below. Additionally, the scene was illuminated using infrared LED panels (940 nm panel, Cop Security). A high-speed camera (90 Hz, Grasshopper3-NIR, FLIR Systems) with an infrared filter (R72, Hoya) was used to track the larva's centroid position in real-time (**Fig. 1A**).

Two virtual light intensity landscapes were used: a "Valley" stimulus (for experimental trials) and a "Constant" stimulus (for control trials). For the "Valley" stimulus, the spatially uniform light intensity (λ) was updated according to $\lambda = (r-3)^2/9$, where r is the larva's radial distance to the center of the arena (**Fig. 1B**). We chose this profile because high luminance levels near the wall decreased the edge preference of larvae. For the "Constant" stimulus, we chose $\lambda = 0.5$, regardless of the larva's position. Both experimental and control trials lasted for 60 min. We also included a 15 min acclimation period before the trials, during which larvae were presented with constant light intensity at an intermediate level ($\lambda = 0.5$), allowing them to distribute in the arena.

Data analysis and statistics

All data analysis was performed using custom-written Python and MATLAB code. Although the temporal phototaxis effect was observed during the entire 60 min period, we found that the effect decreased over the course of the experiment (**Fig. S1A**). Therefore, we only analyzed the first 20 min of behavior data. To avoid tracking problems for the detailed analysis of speed as well as turn events, we excluded all data where larvae was within 0.3 cm of the edge (approximately one body length).

To detect turn events (**Fig. 2A**), we smoothed all position data over a 3 s window, then calculated the instantaneous angular change by taking the angular change between three consecutive positions at 1/90s intervals. Turn events were empirically determined to have instantaneous angular changes greater than 7.2 degrees. To analyze turn events, we calculated heading angle change by taking the angle between the direction vectors before and after a turn event. For all location-dependent analyses, the circular arena was binned in three concentric regions depending on the radius r: the "Bright center" ($r = 0 - 2\ cm$), the "Dark ring" ($r = 2 - 4\ cm$), and the "Bright edge" ($r = 4 - 6\ cm$). According to the respective brightness profile (**Fig. 1B**), the "Bright center" and the "Bright edge" were also defined as the "Bright" regions, whereas the "Dark ring" was also defined as the "Dark" region (**Fig. 2D,F**). Notably, as a control, we always applied the same "Dark"/"Bright" binning and nomenclature to larvae which were presented with the "Constant" stimulus, even though the arena remained constantly gray for those animals.

For pairwise comparisons between the experimental and control data ("Valley" and "Constant" stimuli), we used two-sample t-tests. For pairwise comparisons within groups, we used paired-sample t-tests. If larvae did not move during the experiment or if they spent most of the time near the edge, we discarded this data. All data analysis was done automatically in the same way for the experimental and control groups.

Modeling

Simulations were custom-written in MATLAB. We constructed a simple algorithmic model where larvae behave like randomly moving particles with occasional turn events. Model larvae started at a random position in the arena and with a random direction vector, moving at a speed of 0.41 cm/s, the average running speed of larvae as found in our experiments (**Fig. 1F**). Simulations were performed using a loop with a timestep of $dt = 0.1\ s$. At each time step, larvae stochastically chose one of two possible actions. With a probability of $p = 0.01$, they performed a turn event and changed their direction vector by ±50°, the measured average heading angle (**Fig. 2B,C**). This probability was chosen to approximate the experimentally found inter-turn event interval (~10–15 s; **Fig. S2A**). Otherwise, larvae changed their heading by only ±5°, mimicking the properties of a randomly diffusing particle during runs. Edge preference was included in the model as well: if larvae reached the edge, they remained there for 10 seconds, and then chose a new random direction vector.

In correspondence with our measured behavioral data, our model included three additional navigational rules: In "Rule 1", the magnitude of a heading angle change ω depends on the current

luminance (**Fig. 2B**). If a turn event occurred in the "Dark", the heading angle change magnitude (baseline = ±50°) was reduced by 5°. If it occurred in a "Bright" region, it was increased by 5°. In "Rule 2", the magnitude of the heading angle change ω depends on the change in light intensity since the previous turn event (**Fig. 2C**). If luminance had decreased since the last turn event ($\Delta\lambda < 0$), the magnitude of the heading angle change ω was reduced by 5°. Otherwise ($\Delta\lambda > 0$), it was increased by 5°. In "Rule 3", the probability of initiating a turn event depends on the luminance change since the previous turn (**Fig. 2E**). If brightness had decreased ($\Delta\lambda < 0$), the probability was lowered to $p = 0.005$. If brightness had increased since the last turn ($\Delta\lambda > 0$), the probability was increased to $p = 0.1$. These changes in the magnitude of the heading angle change ω and the turn event initiation probability were allowed to be additive for combinations of the three rules. All eight combinations of these rules were tested (**Fig. 3C–G**), and the performance of each model was ranked using a phototaxis index (**Fig. 3H**). The phototaxis index is defined as $PI = (f_{exp} - f_{control}) / 0.5 \cdot (f_{exp} + f_{control}) \cdot 100$, where f_{exp} and $f_{control}$ are the fractions of time the experimental and control groups spent in the "Dark ring". For the phototaxis index calculation – which depends on the difference between two independent groups – means and variances were determined by randomly sampling difference values 1000 times (bootstrapping). For all of the navigational models, n = 25 simulated larvae navigated the "Valley" stimulus and the "Constant" stimulus.

Results

Fly larvae can navigate a virtual luminance gradient

We first wanted to know whether fly larvae can perform purely temporal phototaxis, i.e. whether they can navigate a virtual light landscape in the absence of any spatial information. We placed individual larvae in a transparent dish filled with agarose and tracked their position in real-time (**Fig. 1A**). We used a projector to present spatially uniform light from below and coupled luminance levels to the larva's position in the arena in a closed-loop configuration. To test the animal's ability to perform phototaxis using only temporal changes in luminance, we created a stimulus where the global brightness level followed a quadratic dependence of the larva's radial distance from the center. This stimulus generated a virtual "Valley" in which a dark ring lies in between two bright regions (**Fig. 1B**). To control for naive location preference, we also tested a "Constant" stimulus in which luminance levels always remained gray, irrespective of the position of the larva. Notably, for both "Valley" and "Constant" stimuli, luminance values were always homogeneous across space, completely removing any spatial contrast that animals might use during navigation. After an initial period of presentation of constant gray, we allowed larvae to navigate either the "Valley" or the "Constant" stimulus for 60 minutes and analyzed their distribution across three concentric regions: the "Bright" center; the "Dark" ring; and the "Bright" edge.

At the beginning of each trial, larvae from both groups were mostly found near the "Bright" edge region (**Fig. 1C** and **Fig. S1A**), which is consistent with their innate edge preference. However, at the end of the trial, larvae that had navigated the "Valley" stimulus mostly accumulated in the "Dark" ring region while larvae that had navigated the "Constant" stimulus remained in the "Bright" edge region (**Fig. 1C**). These differences between the two groups were also visible in the raw trajectories of larvae during the time course of the experiment (**Fig. 1D**). Further, quantifying the amount of time each larvae spent in the three regions revealed that animal's navigating the "Valley" stimulus spent a significantly higher fraction of time in the dark ring than those crawling in the "Constant" stimulus (**Fig. 1E**). Notably, while navigating the virtual "Valley" stimulus, larvae have no spatial luminance cues, posing the question of which behavioral algorithms they might employ. One possible explanation is that larvae simply modulate their crawling speed as a function of luminance – if larvae slow down when the environment is dark, the fraction of time spent in darker areas would be higher. To test this idea, we analyzed crawling speed for the different regions, which revealed that this feature is independent of luminance (**Fig. 1F**), suggesting that larvae seem to employ more complex navigational strategies.

In summary, we conclude that *Drosophila* larvae are capable of performing temporal phototaxis in the absence of any spatial information and that this behavior cannot be explained by a simple luminance-dependent modulation of crawling speed.

Larval temporal phototaxis depends on light level history

In spatially differentiated light landscapes, fly larvae are known to make movement decisions by casting their head back and forth during turn events to sample luminance differences (Humberg and Sprecher, 2018; Humberg et al., 2018; Kane et al., 2013; Lahiri et al., 2011). However, this strategy cannot explain the results in our temporal phototaxis assay because larvae remain at the same position during turn events and, hence, they do not experience any spatial or temporal brightness fluctuations. An alternative strategy that larvae might employ is to modulate the magnitude and/or the frequency of turn events as a function of luminance. To explore this possibility, we first sought to quantify turn events in more detail (**Fig. 2A**). In a first set of analyses, we found that during turn events the heading angle changes were slightly larger when larvae were exposed to bright whole-field luminance compared to when they were in darkness (**Fig. 2B**).

We also sought to test whether the history of luminance change might affect the behavior. As the length of run periods between turn events was highly variable, ranging from ~3 s to up to ~40 s (**Fig. S2A**), we focused on the experienced luminance change in between two consecutive turn events. Accordingly, we grouped turn events by whether larvae had experienced an overall decrease or increase in whole-field luminance during the previous run. We found that heading angle changes were larger when larvae had experienced an increase in brightness compared to when they had experienced a decrease (**Fig. 2C**).

Larvae are known to initiate turn events in response to sudden brightness changes (Kane et al., 2013). We, therefore, next wanted to investigate the possibility that slow luminance changes experienced during runs might also modulate the probability of initiating turn events. We first measured the run time when animals ended in darkness or brightness, which revealed no relationship (**Fig. 2D**). We then grouped turn events according to whether larvae experienced an overall decrease or increase in whole-field luminance since the previous turn event. We found that run times were significantly longer for periods of luminance decrease compared to periods of luminance increase (**Fig. 2E**). The magnitude of such luminance changes during runs was indeed high, on the order of ~10 % of the contrast range in our projection system (**Fig. 2F**), whereas luminance changes within turn events were negligible (**Fig. 2G**). These observations led us to

hypothesize that larvae might accumulate information about the change in luminance during runs and that the respective integration times might span several seconds (Gepner et al., 2015).

In summary, through analyzing turn events and run times, we find that larvae slightly modulate the magnitude of heading angle changes as a function of luminance. Moreover, during runs, they seem to be able to accumulate luminance change and might use such information to modulate heading angle changes as well as the probability to initiate turns.

A simple algorithmic model can explain larval temporal phototaxis

We next wanted to know if the identified behavioral features are sufficient to explain larval temporal phototaxis. Based on our experimental findings, we propose three navigational rules which larvae might use as navigational strategies during phototaxis (**Fig. 3A**): In “Rule 1”, the heading angle change after a turn event is lower if the turn event occurs when it is dark and higher when it is bright (based on **Fig. 2B**). In “Rule 2”, the heading angle change is lower if larvae had experienced a luminance decrease during the previous run and higher if luminance had increased (based on **Fig. 2C**). In “Rule 3”, the probability to initiate a turn event is lower when the current luminance is lower than the luminance at the beginning of a run, and higher when the current luminance is higher (based on **Fig. 2E**).

In order to test these navigational rules, we designed a simple algorithmic model in which larvae behaved like randomly moving particles with occasional changes in heading direction. We allowed model larvae to navigate the same virtual luminance landscapes that we used in the experiments – the “Valley” stimulus and the “Constant” stimulus – and analyzed the resulting trajectories. Consistent with our hypothesis, when all three rules were active, model larvae tended to move towards darker regions, whereas they did not do so in the absence of these rules or for the control stimulus (**Fig. 3B**), as we found in the experiments (**Fig. 1C**). To quantify these effects for different combinations of the proposed navigational rules, we measured the time spent within each region, as we did for our experimental data (**Fig. 1E**). As expected, without these rules, the distribution of larvae in the “Valley” stimulus was the same as for the “Constant” stimulus (**Fig. 3C**). Interestingly, adding “Rule 1” or “Rule 2” to our model was insufficient to produce the observed behavior (**Fig. 3D,E**), suggesting that modulating the heading angle change alone cannot explain temporal phototaxis. We next tested “Rule 3” and found that model larvae were now able to find the “Dark” ring region (**Fig. 3F**) – as was the case when we combined all three navigational rules (**Fig. 3G**) – suggesting that altering the probability of initiating a turn event is critical for temporal phototaxis. Finally, in order to compare the performances of all eight

combinations of the navigational rules, we calculated a phototaxis index, defined to be the difference of time spent in the “Dark” ring between experimental and control groups (**Fig. 3H**). We found that all models without “Rule 3” failed to reproduce the behavior, but any model using “Rule 3” worked well. Using a combination of “Rule 2” and “Rule 3” further improved the phototaxis index. A combination of all three rules led to performance approaching the experimentally observed value.

Finally, even though we did not find this feature in our experiments (**Fig. 2D**), we tested if larval temporal phototaxis could be explained by increasing the probability of initiating a turn event when the environment is bright and decreasing it when the environment is dark. We incorporated this idea as “Rule 4” in our model and found that this navigational strategy could not explain the observed behavior (**Fig. S3A**).

In summary, after implementing the experimentally observed navigational rules in a simple computational model, we propose that the most critical element of larval temporal phototaxis is their ability to adjust their turn event probability as a function of luminance change.

Discussion

Demonstrating the ability of *Drosophila* larvae to engage in temporal phototaxis is critical to understanding how these animals navigate in natural environments, which are dominated by gradual rather than sharp luminance changes. Using our novel, closed-loop behavioral assay, we show that *Drosophila* larvae can find the darker regions of a continuous, always spatially uniform luminance landscape (**Fig. 1E**). Previous research has shown that larvae increase their heading angle change magnitude and the frequency of turn events in response to increases in spatially uniform luminance (Humberg et al., 2018; Kane et al., 2013). We show that larvae are actually capable of using these behavioral strategies to navigate spatially uniform environments. Using a simple computational model, we further demonstrate that modulating heading angle change magnitude (**Fig. 2C**) and the probability to initiate turn events (**Fig. 2E**) is sufficient to reproduce a considerable amount of the temporal phototaxis behavior (**Fig. 3H**). Based on the results from our computational model, as well as based on previous work (Gepner et al., 2015; Gomez-Marin et al., 2011), we suggest that the relevant integration times of luminance change are in the order of multiple seconds. Characterization of the precise time scale and the dynamics of such an integrator system will, however, require additional behavioral experiments.

The wide array of genetic and molecular tools available for manipulating *Drosophila* invite future studies of the neural circuitry underlying phototaxis behavior. Manipulation experiments have already identified specific photoreceptor pathways involved in the processing of temporal luminance cues (Humberg and Sprecher, 2018; Humberg et al., 2018). To characterize these circuits further and to identify potential downstream targets, experiments involving functional imaging of larger neuronal populations in immobilized animals, as well as more precise circuit manipulations in combination with behavior, are needed (Hernandez-Nunez et al., 2015). The design of such experiments will benefit from the existing knowledge of the precise wiring diagram of the early fly larval visual system (Larderet et al., 2017).

Understanding larval phototaxis under more natural conditions requires the study of both the temporal and spatial components of the underlying computations (Humberg et al., 2018). However, the spatial component is technically more difficult to study in isolation than the temporal component. In previous studies, even though larvae navigated spatially differentiated landscapes, one cannot rule out the possibility that larvae might use temporal comparisons of light intensity during turn events (Humberg et al., 2018; Kane et al., 2013). To the best of our knowledge, pure spatial phototaxis has so far only been studied in zebrafish larvae (Huang et al., 2013). Here, spatially locking a sharp contrast edge to the center of the head of a freely moving animal removes

any temporal fluctuations of luminance from the perspective of the animal. Testing such paradigms in *Drosophila* larvae will require more precise measurements of the position, orientation, and posture of the animal in real-time. The results from such experiments could then be used to construct a behavioral spatial phototaxis model which could then be combined with our proposed temporal phototaxis model.

Acknowledgments

We thank L. Hernandez-Nunez for discussions and reading through the manuscript. We are grateful to F. Engert and A. Samuel and their lab members for discussions and general support.

Author contributions

All authors contributed equally to the design of the project. A.B. built the behavioral setup. M.Z. performed experiments and analyzed data. M.Z. and A.B. wrote the manuscript with contributions from all other authors. K.J.H., K.V., and A.B. supervised the work.

Competing interests

The authors declare no competing interests.

Funding

K.J.H. was funded by the Harvard Mind Brain Behavior Initiative. K.V. received funding from a German Science Foundation Research Fellowship #345729665. A.B. was supported by the Human Frontier Science Program Long-Term Fellowship LT000626/2016.

Data availability

The data that support the findings of this study are available from the corresponding author upon request. Source code for data analysis and algorithmic modeling will be made available on GitHub.

References

Bahl, A. and Engert, F. (2020). Neural circuits for evidence accumulation and decision making in larval zebrafish. *Nat. Neurosci.* **23**, 94–102.

Chen, X. and Engert, F. (2014). Navigational strategies underlying phototaxis in larval zebrafish. *Front. Syst. Neurosci.* **8**, 1–13.

Gepner, R., Mihovilovic Skanata, M., Bernat, N. M., Kaplow, M. and Gershow, M. (2015). Computations underlying Drosophila photo-taxis, odor-taxis, and multi-sensory integration. *Elife* **4**, 1–21.

Gomez-Marin, A. and Louis, M. (2012). Active sensation during orientation behavior in the Drosophila larva: more sense than luck. *Curr. Opin. Neurobiol.* **22**, 208–215.

Gomez-Marin, A. and Louis, M. (2014). Multilevel control of run orientation in Drosophila larval chemotaxis. *Front. Behav. Neurosci.* **8**, 1–14.

Gomez-Marin, A., Stephens, G. J. and Louis, M. (2011). Active sampling and decision making in Drosophila chemotaxis. *Nat. Commun.* **2**, 1–10.

Hernandez-Nunez, L., Belina, J., Klein, M., Si, G., Claus, L., Carlson, J. R. and Samuel, A. D. T. (2015). Reverse-correlation analysis of navigation dynamics in Drosophila larva using optogenetics. *Elife* **4**, 1–16.

Huang, K.-H., Ahrens, M. B., Dunn, T. W. and Engert, F. (2013). Spinal projection neurons control turning behaviors in zebrafish. *Curr. Biol.* **23**, 1566–1573.

Humberg, T.-H. and Sprecher, S. G. (2018). Two pairs of Drosophila central brain neurons mediate larval navigational strategies based on temporal light information processing. *Front. Behav. Neurosci.* **12**, 1–6.

Humberg, T.-H., Bruegger, P., Afonso, B., Zlatic, M., Truman, J. W., Gershow, M., Samuel, A. and Sprecher, S. G. (2018). Dedicated photoreceptor pathways in Drosophila larvae mediate navigation by processing either spatial or temporal cues. *Nat. Commun.* **9**, 1–16.

Kane, E. A., Gershow, M., Afonso, B., Larderet, I., Klein, M., Carter, A. R., de Bivort, B. L., Sprecher, S. G. and Samuel, A. D. T. (2013). Sensorimotor structure of Drosophila larva phototaxis. *Proc. Natl. Acad. Sci. U.S.A.* **110**, 3868–3877.

Klein, M., Afonso, B., Vonner, A. J., Hernandez-Nunez, L., Berck, M., Tabone, C. J., Kane, E. A., Pieribone, V. A., Nitabach, M. N., Cardona, A., et al. (2015). Sensory determinants

of behavioral dynamics in Drosophila thermotaxis. *Proc. Natl. Acad. Sci. U.S.A.* **112**, 220–229.

Lahiri, S., Shen, K., Klein, M., Tang, A., Kane, E., Gershow, M., Garrity, P. and Samuel, A. D. T. (2011). Two alternating motor programs drive navigation in Drosophila larva. *PLoS One* **6**, 1–12.

Larderet, I., Fritsch, P. M. J., Gendre, N., Neagu-Maier, G. L., Fetter, R. D., Schneider-Mizell, C. M., Truman, J. W., Zlatic, M., Cardona, A. and Sprecher, S. G. (2017). Organization of the Drosophila larval visual circuit. *Elife* **6**, 1–23.

Luo, L., Gershow, M., Rosenzweig, M., Kang, K., Fang-Yen, C., Garrity, P. A. and Samuel, A. D. T. (2010). Navigational decision making in Drosophila thermotaxis. *J. Neurosci.* **30**, 4261–4272.

Mazzoni, E. O., Desplan, C. and Blau, J. (2005). Circadian pacemaker neurons transmit and modulate visual information to control a rapid behavioral response. *Neuron* **45**, 293–300.

Sawin, E. P., Harris, L. R., Campos, A. R. and Sokolowski, M. B. (1994). Sensorimotor transformation from light reception to phototactic behavior in Drosophila larvae (Diptera: Drosophilidae). *J. Insect Behav.* **7**, 553–567.

Figures

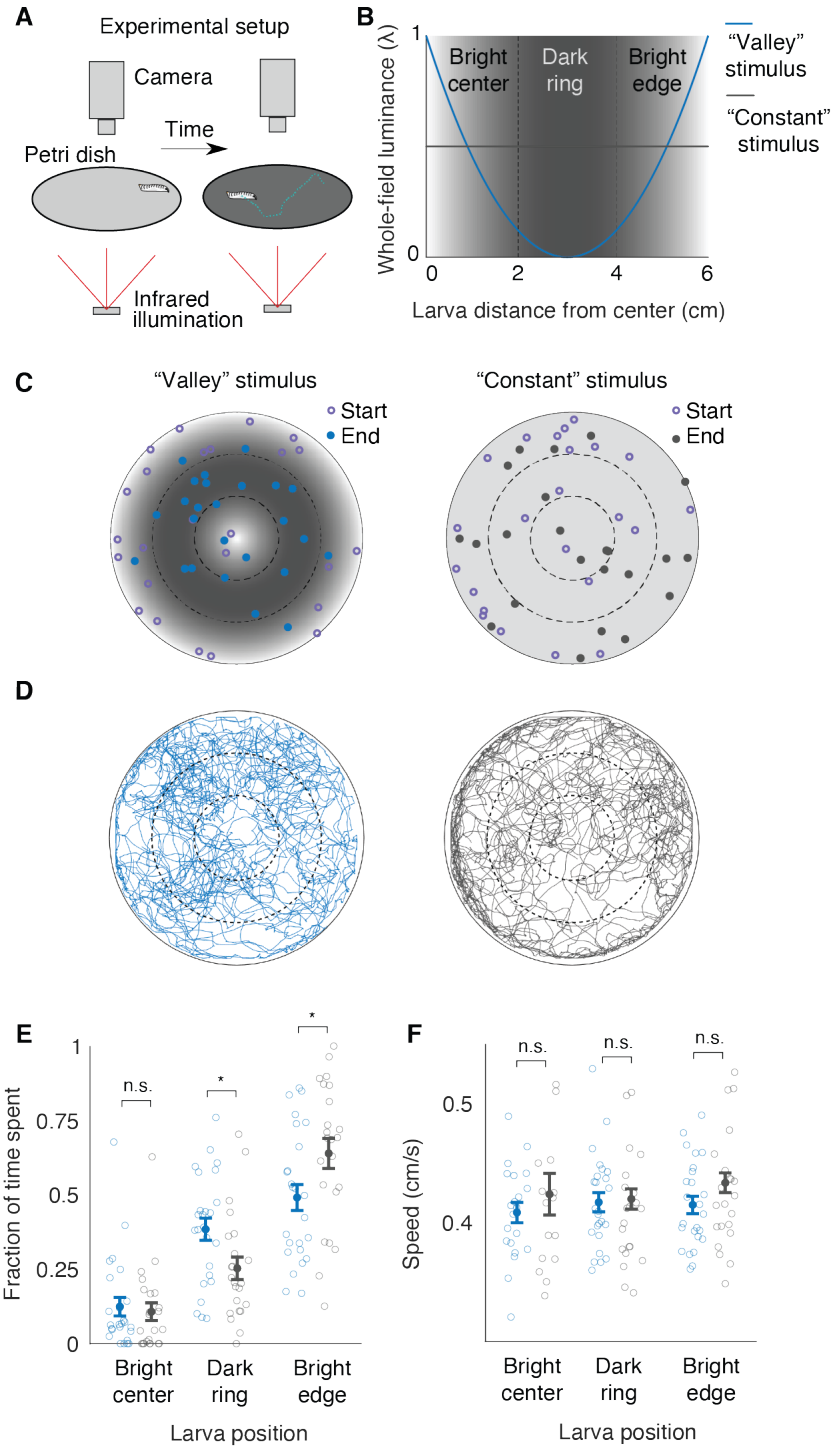

Figure 1 | *Drosophila* larvae can perform temporal phototaxis. (**A**) Experimental setup. The high-speed camera tracks the position of the freely crawling *Drosophila* larva (blue), using infrared illumination (red). A projector presents whole-field illumination to the animal from below. In all experiments, visual stimuli are always spatially uniform. (**B**) For the "Valley" stimulus, the light intensity (λ; blue solid line) is given by $\lambda =$

$(r-3)^2/9$, where r is the larva's radial distance to the center of the arena. For the "Constant" stimulus (gray solid line), λ was set to 0.5 regardless of the larva's position. For all analyses, the arena is split into three concentric regions: the "Bright center" ($r = 0-2\ cm$), the "Dark ring" ($r = 2-4\ cm$), and the "Bright edge" ($r = 4-6\ cm$). (**C,D**) Start and end positions as well as raw trajectories for the "Valley" (left panels) and the "Constant" stimulus (right panels); n = 25 larvae for the "Valley" stimulus and n = 23 larvae for the "Constant" stimulus. (**E,F**) Blue indicates "Valley" stimulus larvae; gray indicates "Constant" stimulus larvae. Open circles represent individual animals. (**E**) Fraction of time larvae spent in each region during the experiment. "Valley" stimulus larvae spent more time in the "Dark ring" region (p = 0.017, two-sided t-test) and less time in "Bright edge" region than "Constant" stimulus larvae (p = 0.031, two-sided t-test); n = 25 larvae for the "Valley" stimulus and n = 23 larvae for the "Constant" stimulus. (**F**) Average speed of larvae for the "Valley" stimulus and for the "Constant" stimulus (n.s. = not significant; p = 0.40, p = 0.86, p = 0.19 from left to right; two-sided t-tests). Note that not all larvae entered all regions during the experiment. For the "Valley" stimulus, out of n = 25 larvae, only 21 animals entered the "Bright center" and all 25 animals entered the other regions. For the control stimulus, out of n = 23 larvae, 16 animals entered the "Bright center" region, 22 animals entered the "Dark ring" region, and all 23 animals entered the "Bright edge" region. Error bars in (**E,F**) represent mean ± SEM.

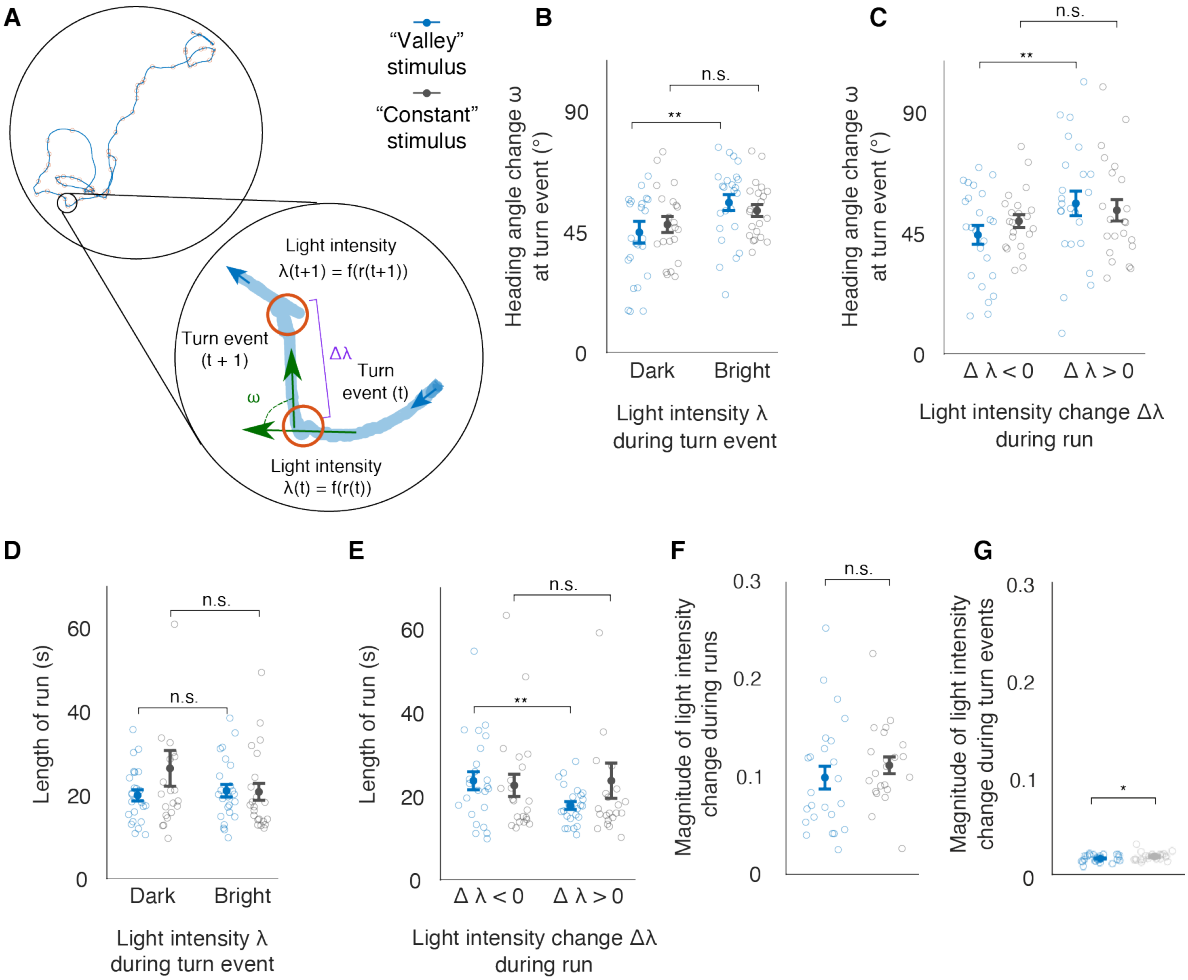

Figure 2 | Brightness, as well as brightness history, modulate behavioral decisions. (**A**) Sample larva trajectory (blue) and detected turn events (red circles). Inset shows two turn events at time *t* and time *t + 1*. The intensity of the spatially uniform whole-field luminance (λ) is a function of the larva's distance from the center. The green arrows indicate the heading angle change (ω) during the turn event. The purple bracket is the change in light intensity during the run. (**B–F**) Blue and gray indicate "Valley" and "Constant" stimulus larvae, respectively. Open circles represent individual larvae. (**B**) Heading angle change at turn events as a function of current light intensity λ. For "Dark" and "Bright": n = 24 and 24 larvae for the "Valley" stimulus and n = 21 and 22 larvae for the "Constant stimulus. (**C**) Heading angle change at turn event grouped based on whether luminance has increased or decreased during the previous run. For Δλ < 0 and Δλ > 0: n = 24 and 24 larvae for the "Valley" stimulus and n = 23 and 23 larvae for the "Constant" stimulus. (**D**) Length of runs as a function of current light intensity. For "Dark" and "Bright": n = 24 and 24 larvae for the "Valley" stimulus and n = 22 and 22 larvae for the "Constant stimulus. (**E**) Length of runs grouped based on whether luminance has increased or decreased during the run. For Δλ < 0 and Δλ > 0: n = 24 and 24 larvae for the "Valley" stimulus and n = 22 and 22 larvae for the "Constant" stimulus. "Dark" means that larvae were located within the "Dark" ring region. "Bright" indicates that larvae were located in the "Bright" center or the

"Bright" edge regions. Note that for the "Constant" control stimulus, the same regional binning nomenclature was used, even though animals always experience intermediate gray luminance levels. (**F**) Magnitude of light intensity change during runs ($p = 0.26$, two-sided t-test). Values represent fraction of stimulus contrast (0 to 255). (**G**) Magnitude of light intensity change during turn events. ($p = 0.027$, two-sided t-test). Error bars indicate mean ± SEM.

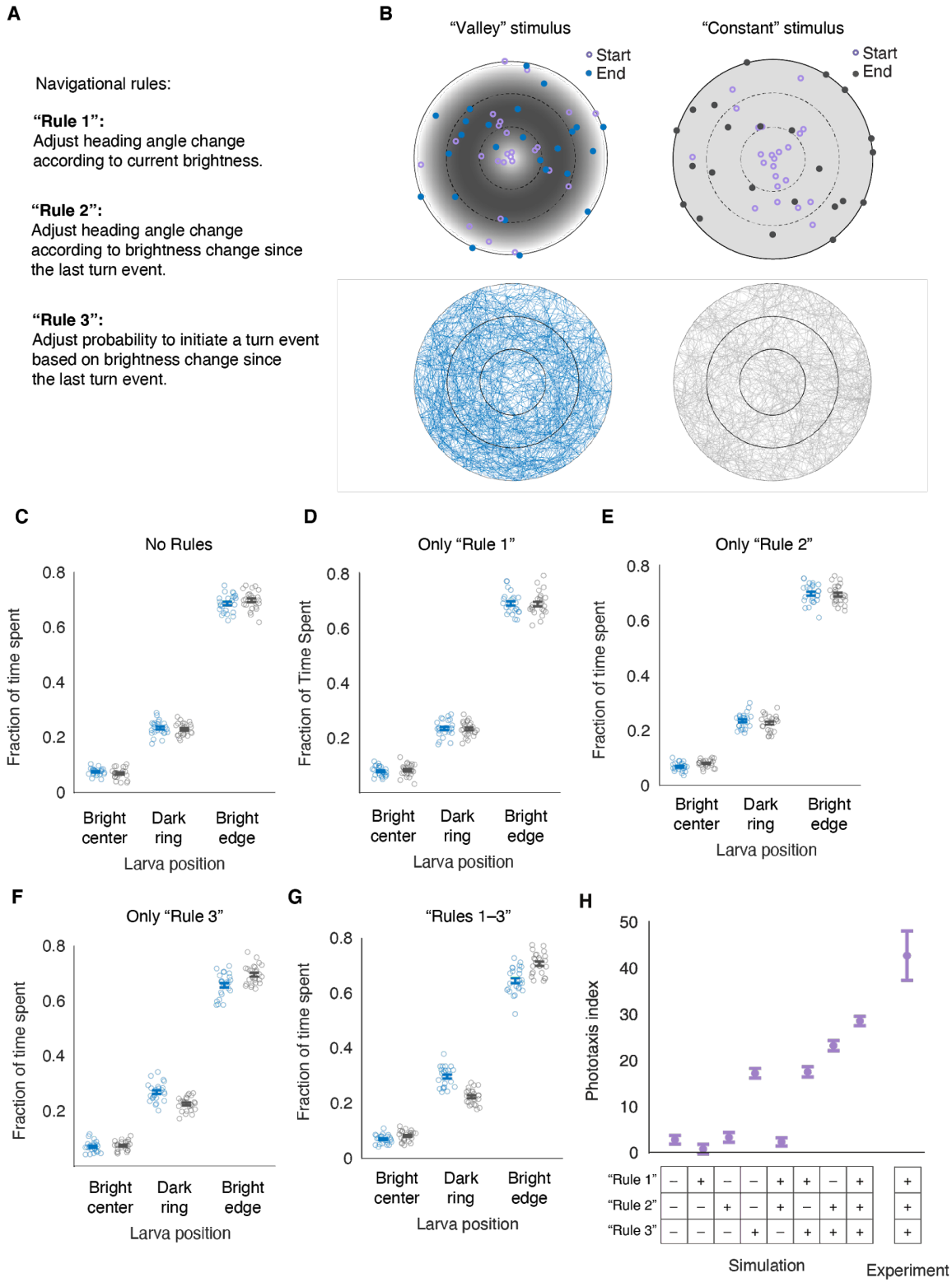

Figure 3 | Simulated larvae can perform temporal phototaxis using three simple navigational rules. (**A**) Description of three navigational rules larvae might use during temporal phototaxis. (**B**) Simulated larvae employing all three rules for the "Valley" stimulus (left) and "Constant" stimulus (right). Start and end

positions (top) and raw trajectories (bottom). (**C–G**). Average fraction of time simulated larvae spent in each region for different combinations of the three navigational rules. Blue and gray indicate “Valley” stimulus and “Constant” stimulus; n = 25 simulated larvae. Error bars represent mean ± SEM. (**H**) Phototaxis index, comparing the eight simulated models with the experimental data. Because the phototaxis index is based on bootstrapped group differences, error bars indicate mean ± 95% confidence interval.

Supplementary figures

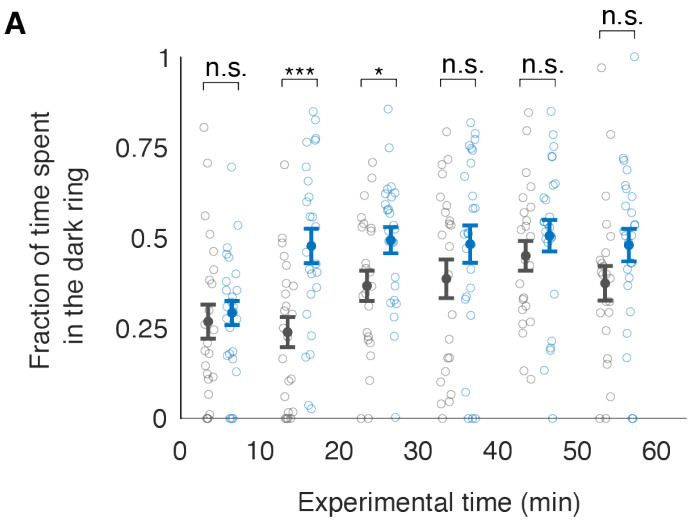

Supplementary Figure S1 | Behavioral performance over the time course of the entire experiment following the 15 min acclimatization period. (**A**). Fraction of time spent in the "Dark ring" region, in 10-minute intervals of the experimental period; n = 25 for the "Valley" stimulus; n = 23 for the "Constant" stimulus. *p < 0.05, ***p < 0.001 (two-sided t-tests). Blue indicates "Valley" stimulus larvae; gray indicates "Constant" stimulus larvae. Open circles represent individual animals. Error bars represent mean ± SEM.

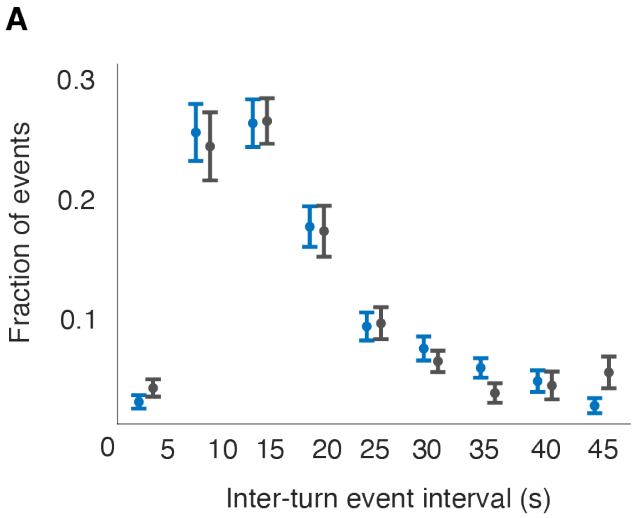

Supplementary Figure S2 | Run-length distribution. (A) Blue indicates "Valley" stimulus larvae; gray indicates "Constant" stimulus larvae. Open circles represent individual animals. N = 25 larvae for the "Valley" stimulus and n = 23 larvae for the "Constant" stimulus. Same animals as in **Fig. 1E**.

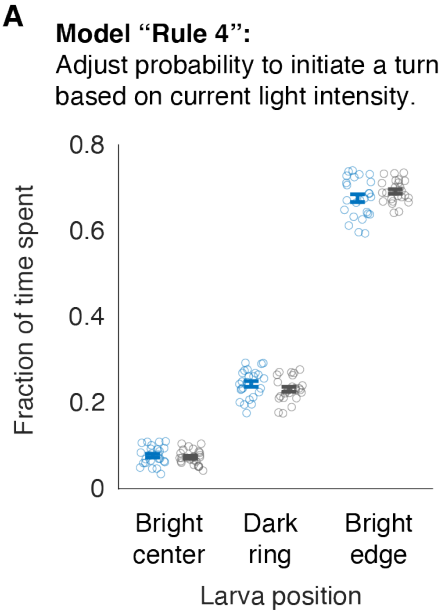

Supplementary Figure S3 | Simulated larvae using a fourth navigational rule. (**A**) Fraction of time simulated larvae spent in each region when using "Rule 4". In "Rule 4", we adjust the probability of initiating a turn as a function of the current light intensity. Blue and gray dots indicate simulated larvae navigating the "Valley" stimulus and the "Constant" stimulus, respectively; n = 25 simulated larvae. Error bars represent mean ± SEM.